

General double monodromy inflation

Guido D’Amico^{1,2,*}, Nemanja Kaloper^{3,†} and Alexander Westphal^{4,‡}

¹*Department of Mathematical, Physical and Computer Sciences, University of Parma, 43124 Parma, Italy*

²*INFN Gruppo Collegato di Parma, 43124 Parma, Italy*

³*QMAP, Department of Physics and Astronomy, University of California Davis, California 95616, USA*

⁴*Deutsches Elektronen-Synchrotron DESY, Notkestrasse 85, D-22607 Hamburg, Germany*



(Received 31 January 2022; accepted 8 April 2022; published 19 May 2022)

We revisit the roller-coaster cosmology based on multiple stages of monodromy inflation. Working within the framework of effective flux monodromy field theory, we include the full range of strong coupling corrections to the inflaton sector. We find that flattened potentials $V \sim \phi^p + \dots$ with $p \lesssim 1/2$, limited to $N \lesssim 25 - 40$ e -folds in the first stage of inflation, continue to fit the cosmic microwave background. They yield $0.96 \lesssim n_s \lesssim 0.97$ and produce relic gravity waves with $0.006 \lesssim r \lesssim 0.035$, in full agreement with the most recent bounds from BICEP/Keck. The nonlinear derivative corrections generated by strong dynamics in effective field theory (EFT) also lead to equilateral non-Gaussianity $f_{\text{NL}}^{\text{eq}} \simeq \mathcal{O}(1) - \mathcal{O}(10)$, close to the current observational bounds. Finally, in the multistage roller coaster, an inflaton–hidden sector $U(1)$ coupling can produce a tachyonic chiral vector background, which converts rapidly into tensors during the short interruption by matter domination. The produced stochastic gravity waves are chiral, and so they may be clearly identifiable by gravity wave instruments like LISA, Big Bang Observer, Einstein Telescope, NANOgrav, or SKA, depending on the precise model realization. We also point out that the current attempts to resolve the H_0 tension using early dark energy generically raise n_s . This might significantly alter the impact of BICEP/Keck data on models of inflation.

DOI: [10.1103/PhysRevD.105.103527](https://doi.org/10.1103/PhysRevD.105.103527)

I. INTRODUCTION

In this article, we complete the analysis of the observable predictions of interrupted monodromy inflation models which we initiated in Ref. [1]. Our goal is to obtain the complete set of observables for monodromy models in strong coupling limit, which in addition to flattened inflaton potentials also include higher derivative operators which renormalize the inflaton’s (inflatons’) kinetic terms. While these corrections yield additional suppression of the tensor-to-scalar ratio r , they tend to push the scalar spectral index n_s closer to unity [1–3]. That might tempt one to interpret the data as a serious obstacle for monodromy models, due to quite tight bounds on r and n_s , $r \lesssim 0.035$, and $0.96 < n_s \lesssim 0.97$ [4]. However, as we will show explicitly in this work, such conclusions would be far too premature. On the contrary, when combined with the idea of roller-coaster cosmology [5], monodromy models

which include flattened potentials—possibly due to first-principle constructions [6,7] or generated by field theory strong coupling corrections [8–10], or even in the multifield models—remain perfectly viable candidates to explain all the cosmological observations to date, while simultaneously generating new signatures that can be tested by the next generation of instruments. We should also stress that the spectral index will be lower when many fields move in unison, simulating a single composite inflaton [11–13]. This is because different fields with nearly degenerate masses fall out of slow roll at different times, inducing a small but potentially relevant correction to n_s .

In the present work, the key input will be interrupting inflation at around 20–35 e -folds before the end, by the choice of the multifield potential. The interruption resets the pivot at which the observables are generated and normalized. In turn, this pushes n_s back to lower values and restores consistency with the observations, while simultaneously keeping $r \lesssim 0.035$ thanks to the potential flattening. Even if the first principles constructions generate steeper potentials, the potential flattening induced by strongly coupled physics could be very efficient by itself, thanks to both the “seizing” effect induced by wavefunction renormalization [8–10,14] and to the higher derivatives which further assist by reducing the speed of sound of the perturbations [10]. However, in the latter case, the nonlinear derivative operators simultaneously generate

*damico.guido@gmail.com

†kaloper@physics.ucdavis.edu

‡alexander.westphal@desy.de

Published by the American Physical Society under the terms of the Creative Commons Attribution 4.0 International license. Further distribution of this work must maintain attribution to the author(s) and the published article’s title, journal citation, and DOI. Funded by SCOAP³.

non-Gaussianities that could disrupt the cosmic microwave background (CMB) if they are too large (such phenomena are automatically very suppressed at weak coupling). Suppressing non-Gaussianities yields a lower bound on r , about $r \gtrsim 0.006$, for the models with the flattened potentials $V \sim \phi^p + \dots$, $0.1 \leq p \lesssim 1/2$, which are at the edge of the “penumbra around the lamppost” of the string theory motivated constructions at this time.

Moreover, if the interrupted inflaton, which is an axionlike field, also couples to a dark photon with the decay constant near the scale of inflation, it will generate very large dark photon chiral fields. These in turn source chiral gravity waves, that are frozen out at superhorizon scales during the second stage of inflation, lasting another 20–35 e -folds [1]. These gravity waves present a very strong signal which could be detected by future instruments like, for example, LISA, Big Bang Observer, Einstein Telescope, NANOgrav, or SKA, depending on the precise details of the models and the scales which they require, or rather where the stages of inflation are interrupted. This makes our specific subclass of strongly coupled EFT monodromy models particularly interesting, since their signatures are within reach of the multiple near-future observations.

To proceed, in the next section, we will discuss how to include the higher derivative corrections induced at strong coupling and reanalyze their effects on the background dynamics of inflation and on perturbations. Solving the equations numerically, we will fit the results against the most recent BICEP/Keck data [4], confirming the assertions above that they fit CMB, interpreted within the Λ CDM “concordance model” of late cosmology, perfectly, with $0.96 \lesssim n_s \lesssim 0.97$ and $0.006 \lesssim r \lesssim 0.035$, when the first stage of inflation is interrupted a few decades of e -folds before the end.

We will then show how the lower bound on r comes about due to the combination of non-Gaussianities induced by the higher derivatives terms and the assumption that $p \geq 0.1$. We impose this condition to stay near the range of parameters that can be related to explicit string theory motivated corrections. We will also use a toy model of a theory with higher derivative operators to illustrate just how significant these effects can be.

In Sec. III, we will revisit the mechanism for chiral gravity wave production, described in Ref. [1]. We will explain that the results transfer straightforwardly from the previous case, where we neglected the higher derivatives, because by the time the first stage of inflation ends the inflaton sector is in weak coupling. We will see that for powers $1/2 \geq p \geq 0.25$, the interruption pivot occurs at ~ 20 – 35 e -folds of inflation before the end. Hence, for those cases, the produced primordial gravity waves are in the range of LISA or DECIGO. If powers are lower, $0.25 \geq p \geq 0.1$, inflation may need to end sooner, implying that the produced chiral gravity waves could have larger wavelength, and might be in the range of SKA or NANOgrav, or other instruments.

Finally, we will also stress a rather curious and unexpected connection between the problem of constraining the early Universe cosmology and inflation and the determination of the late Universe value of the Hubble parameter H_0 . The Λ CDM “concordance cosmology” may be facing a serious challenge from the intriguing discrepancy in determining H_0 using CMB from that one using supernovae [15–23]. The two values are $H_0 \simeq 68$ km/sec/Mpc and $H_0 \simeq 73.3$ km/sec/Mpc, and according to the latest analyses, this leads to a 5σ disagreement between the two [24]. An interesting interpretation of this problem is that plain vanilla Λ CDM may not be right, and a leading contender which might reconcile the two values of H_0 might be the introduction of a new material in the Universe commonly dubbed “early dark energy” [18,20,21]. Refitting the CMB to the late data, however, seems to require raising the primordial value of n_s . This therefore directly influences the bounds on the early inflation, despite naive expectations that the two regimens, the early and the late Universe, should be “decoupled.” This is not a deep conceptual issue, however, but is a potentially serious practical aspect of early Universe imprint contamination by late Universe evolution and is a familiar issue from early forays into CMB fits [25–28]. We will not dwell on possible resolutions of the H_0 tension here beyond pointing out that the implications for the r versus n_s bounds may be quite dramatic, broadening the range of values for n_s , and ruling “in” models of inflation alleged to have been excluded and severely constraining other models currently touted to be “in good standing.”

Either way, the jury is still out, and we are looking forward to whatever exciting news comes our way.

II. FLEXING THE BICEP OF THE DOUBLE-COASTER

As in Ref. [1], we will work here with a simple two-field model which supports a two-stage inflation that is interrupted before it realizes 60 e -folds. We note that in more general cases, the early Universe could involve more than just two stages of inflation, with multiple inflatons which can leave signatures at many different scales [5]. We will set the details of this more general and interesting possibility aside in this work for the sake of simplicity. However, we will invoke them later, when outlining a range of predictions. It would be interesting to explore such scenarios in further detail. In the two-field case, during the interruption, the first inflaton field oscillates, such that the effective equation of state of the Universe in this epoch is $w \simeq 0$. This reproduces the dynamics considered in the past in Refs. [29–38], albeit at a different pivot relative to the beginning of inflation. Models like this are readily found in monodromy constructions [6,8,39–42], which typically involve more than one field, where the fields are separated by small mass hierarchies.

We recall that there is a range of possible effects which can flatten the potentials without and with strong coupling.

For example, at weak coupling [6,7], integrating out fields heavier than the inflaton may lead to potential flattening as in Ref. [14], and the theory may be under control even in weak coupling. In strong coupling, such effects may be ubiquitous in flux monodromy models [1,10], where the fact that the inflaton is a magnetic dual of a longitudinal helicity of a massive 3-form potential gauge theory [8,41,43] allows gauge symmetry to “cherry-pick” the right kinds of higher-dimension operator corrections, which, while preserving gauge symmetry, generically flatten the potential. In fact, just allowing several fields simultaneously in slow roll, as in assisted inflation/N-flation [44–46], could push the spectral index down [11–13].

Bearing all of the previous elaboration in mind, we will take an “ignoble” approach and develop a model based only on EFT + gauge symmetries. This means we will take each inflaton to be an axionlike field, which is a magnetic dual of a massive 3-form potential gauge theory. For the most part, we will forego the details of the UV completion which we do not have and using gauge symmetries and naturalness push forward to show that the EFT, when allowed to employ strong coupling effects (just) below its cutoff, may yield a successful model of inflation [10,43]. The low energy theory, in effect, is really a theory of gravitating superconductor, advocated in Ref. [43]. With this in mind, we proceed with retaining the potential we used in Ref. [1],

$$V(\phi_1, \phi_2) = M_1^4 \left[\left(1 + \frac{\phi_1^2}{\mu_1^2} \right)^{\frac{p_1}{2}} - 1 \right] + M_2^4 \left[\left(1 + \frac{\phi_2^2}{\mu_2^2} \right)^{\frac{p_2}{2}} - 1 \right]. \quad (1)$$

As before, the scales μ_1, μ_2 normalizing the fields are both $\mathcal{O}(0.1M_{\text{Pl}})$. We take $M_2 \lesssim M_1 \simeq M/\sqrt{4\pi}$, where $M/\sqrt{4\pi}$ is the strong coupling scale of the theory and M is the UV cutoff. We imagine that it is set by the mass of the lightest heavy field which was integrated out to obtain the effective potential (1).

Both ϕ_i are axions arising from truncating p -form gauge potentials in string theory constructions, either as directly p -form components in compact directions or as the magnetic duals of the residual 4-forms.¹ This immediately connects masses and axion decay constants, $\mu_i \sim f_i$. The latter are further bounded by $f \sim M_{\text{Pl}}/(M_s L)^q \lesssim M_{\text{Pl}}$ where L is the size of the compactification cycle giving rise to the relevant axion and M_s is the string scale [47,48]. As a result, f_i is typically of the order of $10^{-2}M_{\text{Pl}} \lesssim f \lesssim M_{\text{Pl}}$, justifying our choice of μ_i . The scales M_i typically arise from warping effects or dilution of energy densities with inverse powers of extra dimension volumes (see, e.g., Sec. IV 1 in Ref. [49] for a summary), which are either power law or exponentially sensitive to the

¹The distinction is important in understanding the origin of higher derivative operators later on.

microscopic parameters in a string compactification. Finally, the axions ϕ_i arise from two mutually sequestered sectors of a given model, only interacting via gravity, and so generically $M_1 \neq M_2$. This also explains why we ignore the mixing between the two axions. Without loss of generality, we take $M_2 \lesssim M_1$.

Next, in this work, we will also include the higher derivative operators which correct the kinetic terms, which as we stressed are unavoidable in the strong coupling regime by naturalness of the perturbation theory [10]. In this regime of the theory, the only way to avoid some of these operators, short of fine-tuning, is if there is some symmetry prohibiting them. Note that in weak coupling, below the cutoff, in explicit constructions, such operators need not play a significant role, while the potential may nevertheless be flattened [6,7], due to the features of the UV completion of the direct string construction. Our point here is that, even without knowing the full details of the string construction and the precise realization of the UV completion, as long as the low energy EFT has gauge symmetries as in flux monodromy [43], some flattening of the potential will happen in strong coupling when the gauge invariant higher-dimension operators are included. As we already stated, this may well be the most conservative approach to the realization of models with flattened potentials, and more efficient means may be found. However, in our view, the merit of our approach is that it *accommodates* the inflationary evolution—just like the London theory of superconductivity accommodated superconducting phenomena decades before Bardeen-Cooper-Schrieffer (BCS). The higher-dimension operators of interest take the form [10]

$$\mathcal{L} \ni \sum_{k \geq 1, l \geq 1} c_{k,l} \frac{(m_j \phi_j)^l}{2^k k! l! \left(\frac{M^2}{4\pi}\right)^{2k+l-2}} (\partial_\mu \phi_j)^{2k}, \quad (2)$$

where $m_i^2 \simeq p_i^2 M_i^4 / \mu_i^2 < M^2$ are the effective inflaton masses in the flattened regime.

We take the powers p_i to be small, $0.1 \lesssim p_i \leq 1$, reflecting the flattening of the potentials due to the interactions with heavy fields which are integrated out [1,7,10]. In the strong coupling regime, we can see how such terms arise by imagining higher-dimension operators $\sim \left(\frac{4\pi\phi_i}{M}\right)^q (\partial\phi_i)^2$ renormalizing the kinetic terms in the strong coupling regime $1 > \phi_i/M \geq 1/4\pi$, and canonically normalizing the fields. Such powers can be realized in string constructions “under the lamppost,” which therefore may be under control.²

²To have a valid EFT, we must have a good description of its vacuum. As field values change, and couplings run, the perturbative vacuum itself will evolve. In UV complete frameworks, one may have a full view of this evolution. In perturbative EFT, we do not always have the benefit of such insight.

The effective action for monodromy composed of (1) and (2) can be symbolically “resummed,”³ yielding for each inflaton

$$\mathcal{L}_i = K(\phi_i, X_i) - V_{\text{eff}}(\phi_i) = \frac{M^4}{16\pi^2} \mathcal{K}\left(\frac{4\pi m_i \phi_i}{M^2}, \frac{16\pi^2 X_i}{M^4}\right) - \frac{M^4}{16\pi^2} \mathcal{V}_{\text{eff}}\left(\frac{4\pi m_i \phi_i}{M^2}\right), \quad (3)$$

where $X_i \equiv -(\partial_\mu \phi_i)^2$, the functions \mathcal{K} , $\mathcal{V}_{\text{eff}} = 16\pi^2 V_{\text{eff}}/M^4$ have Taylor coefficients $\sim \mathcal{O}(1)$, and we normalized the expansion using the strong coupling scale M (which can be thought of as the mass of the lightest particle coupled to ϕ_i which was integrated out). The \mathcal{K} is the kinetic function of the theory, which in the weak coupling reduces to $(-1 + \dots)(\partial\phi)^2/2$.

We have chosen to decouple the two axion sectors from each other for simplicity, and as a result, the early inflationary trajectory and the late inflationary dynamics become two separate stages. Thus, in this limit, we can study the dynamics of inflation as a sequence of two consecutive single-field stages. As noted above, this could happen as a leading approximation in the case when the two sectors mix only gravitationally. As in Ref. [1], we view this as an interrupted N-flation [46], with a larger mass gap between the two inflatons, where one dominates early on and drops out of slow roll well before the other one. Each effective action \mathcal{L}_i is precisely the action of the k-inflation model of Refs. [50,51], with a single-dimensional normalizing scale, and the dimensionless coefficients of $\mathcal{O}(1)$ up to combinatorial factors set by normalizing Feynman diagrams. At strong coupling, where the theory (3) is driven by observations, it is this action which should be deployed to compute inflationary background and observables [10]. In Fig. 1, we illustrate the inflationary trajectory on the potential (1). In the present case, the segments of the trajectory are also affected by the higher derivative operators (2) which we retained.

We also note that an even more extreme reduction of r can occur if the potential \mathcal{V}_{eff} at large ϕ plateaus. In a sense, the change of the potential from convex to concave as the strong coupling regime sets in may be viewed as a beginning of such plateauing. In some cases where additional control tools are present, namely AdS/CFT, and the corrections are enhanced by the presence of many flavors, such potentials could be constructed [9,52]. In the example [9], the resulting effective potential is $\mathcal{V}_{\text{eff}} \sim (1 - \frac{1}{1+(4\pi c m \phi/M^2)^p})$. In this case, the tensor-to-scalar ratio is very small, $r \sim \text{few} \times 10^{-4}$ [9,10]. We will, however, not explore the detailed dynamics of such models here.

³We set aside the convergence issues and take the “sum” to be an asymptotic series.

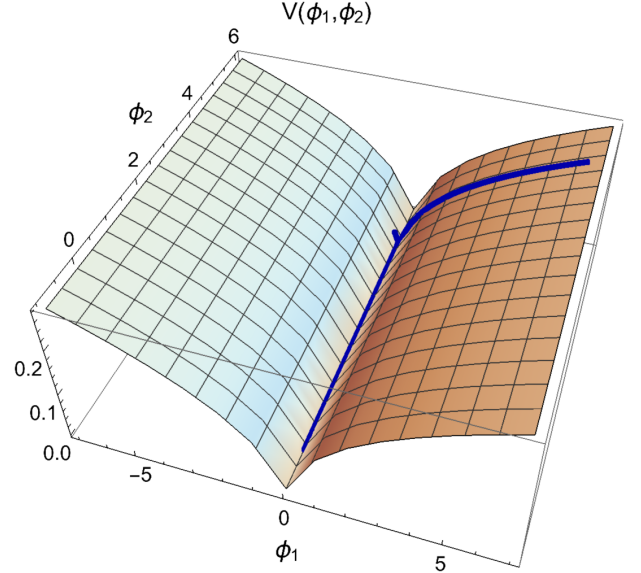


FIG. 1. Two-field potential $V(\phi_1, \phi_2)$ for the model in Eq. (1). Here, $M_1 = 0.5M_{\text{Pl}}$, $M_2/M_1 = 0.1$, $p_1 = 2/5$, $p_2 = 1$, and $\mu_1 = \mu_2 = 0.5$. The blue curve depicts a typical two-stage inflationary trajectory, where the field ϕ_1 slides down the slope first and oscillates while decaying near the bottom of the “gutter” and then ϕ_2 starts to move along the gutter.

The next step is to recalculate the spectrum of perturbations on large scales. As before, we solve the equations of motion for the inflaton and calculate the scalar spectral index n_s and the tensor-to-scalar ratio r at N_e e -folds before the end of the first stage, but now we include the effect of the higher derivative operators. This forces us to resort to numerical integration, and we will only present the result for the first stage of inflation since this is when the fluctuations distorting the CMB are generated. At this stage, we can approximate the dominant contribution to the effective potential during the first stage by

$$V_{\text{eff}}(\phi_1) = M_1^4 \left[\left(1 + \frac{\phi_1^2}{\mu_1^2} \right)^{\frac{p_1}{2}} - 1 \right] \simeq M_1^4 \left[\left(\frac{\phi_1}{\mu_1} \right)^{p_1} - 1 \right], \quad (4)$$

which in the plot of Fig. 1 corresponds to fixing ϕ_2 at some value and rolling down the hill toward the ridge at a $\phi_2 \simeq \text{const.}$, thanks to $\phi_2 \gg \mu_2$. Here, clearly, $M_1 \simeq M/\sqrt{4\pi}$.

In the absence of higher derivative operators in Ref. [1], we could then use the slow-roll parameters $\epsilon_V = \partial_\phi V_{\text{eff}}(\phi_1)^2 / (2V_{\text{eff}}(\phi_1)^2)$ to both control the numerical integration of the dynamics based on (4) in slow-roll regime and to compute the observables $n_s - 1 = 2\eta_V - 6\epsilon_V$, $r = 16\epsilon_V$ at a value of ϕ_1 when the first stage of inflation ends, which gives

$$N_e = \int_{\phi_1}^{\phi_1(\text{end})} d\phi \frac{H}{\dot{\phi}} \simeq \left(\frac{\phi_1^2}{2p_1 M_{\text{Pl}}^2} \right) \left[1 - \frac{2}{2-p_1} \left(\frac{\mu_1}{\phi_1} \right)^{p_1} \right] \quad (5)$$

e -folds before the end of the first inflationary stage. That generated the primordial tensor modes with r in the range $0.02 \lesssim r \lesssim 0.06$ [1].

As noted [10,53], higher derivative operators help reduce r further. In this regime, it is convenient to compute the cosmological observables using the k -inflation approach of Refs. [51,54,55]. Importantly, the speed of sound of the scalar perturbations c_s is different from unity, so that the tensor-to-scalar ratio is $r = 16c_s\epsilon$, and ϵ is the usual slow-roll parameter. In this case, the inflationary consistency relation is $r = -8c_s n_T$, where n_T is the tensor spectral index. What happens is that the higher derivatives improve the slow roll in the scalar field equation, without affecting the gravitational field equations. As a result, the noted modification of the consistency condition follows. Furthermore, the nonlinear terms in the fluctuations [54,55] may yield non-negligible equilateral non-Gaussianities. We will also compute those numerically to show how the non-Gaussianities limit r from below.

To do this, using the calculational framework of k -inflation, we restrict to the subcase when inflation is slow-roll potential driven and require that higher derivative terms dominate over the quadratic ones both in controlling the background and the perturbations. For simplicity, we will present below only the equations for the truncation of the kinetic energy function to only quartic terms, $K = \mathcal{Z}X_1 + \tilde{\mathcal{Z}}\frac{16\pi^2 X_1^2}{M^4}$. We will also consider the sextic derivative terms as an additional example, motivated by direct string theory constructions. Both of these ‘‘transquartic’’ cases suppress r more than the quartic truncations. But in weak coupling, they can go only so far.

III. INTERLUDE WITH HIGH HARMONICS, FOR STRINGS

Before we proceed with computing the observables for the nonlinear theory we have set up so far, let us pause and consider in more detail the origin of the nonlinearities, and in particular the higher derivative terms. The higher derivative operators may arise in the weak coupling limit, in which case their coefficients may be calculable in perturbation theory. Generically, this means the derivative-dependent part of the effective action will be truncated to a few leading terms (as noted in the perturbative analysis in Ref. [53], for example). The leading-order terms are $\propto (\partial)^4$. However, although such terms can indeed arise already at weak coupling in string theory, their impact is limited. In this section, we stipulate what one may expect in the controlled regime under the lamppost, below the strong coupling scale. Our aim is to outline a ‘‘perturbative’’ boundary in the observable phase space and to show by example how strong coupling effects can enhance the observable signals.

Which of the two transquartic cases mentioned above depends on the nature of the underlying monodromy inflaton candidate. If the inflaton scalar arises as a position

modulus of a mobile D-brane acquiring monodromy, e.g., via moving along a nontrivial fibration of the compactification space, its kinetic term may pick up higher-derivative corrections to all orders from the Dirac-Born-Infeld (DBI) action of the moving D-brane generating the inflaton scalar potential as well. As a guiding example, we look, e.g., at the D7-brane monodromy inflation model in Ref. [56] in which the D7-brane position in the transverse extra dimensions is the inflaton candidate. F-theory there allows the authors to describe the D7-brane position as part of the elliptic Calabi-Yau 4-fold complex structure moduli. Therefore, the 7-brane position acquires its two-derivative kinetic term from a Kahler potential in the effective four-dimensional (4D) supergravity.

However, at least in the perturbative type IIB string theory limit of F-theory, this two-derivative kinetic for the D7-brane position is ultimately obtained via matching the expansion of the full DBI action of the D7-brane effective action in Ref. [57] up to two-derivative order. Hence, in the type IIB limit, we expect the full kinetic term of the D7-brane position scalar inflaton candidate for the model of Ref. [56] to take the complete DBI form. We leave a full discussion of these arguments for future work but note that they provide plausibility for the appearance of the full infinite higher-derivative kinetic term series of DBI inflation in brane monodromy inflation setups of schematic type $\sqrt{1 - \alpha' \dot{x}_1^2}$ such as seen, e.g., in Ref. [39], as they rely just on the structure of the DBI action as the universal part of the perturbative effective description of D-branes.

In contrast, if inflation arises as axion monodromy from a bulk p -form string axion, this will not acquire contributions to its kinetic term from branes and thus no DBI-type kinetic term. Instead, the supersymmetric completion of the leading higher-order $\alpha^3 R^4$ [58] curvature correction is expected to generate corrections to the kinetic term of bulk closed string axions up to sextic order from terms containing at least one power of curvature. This expectation arises from considering the supersymmetry (SUSY) completion of the type II $\alpha^3 R^4$ correction. While this completion in its full form is unknown as of today, the bosonic sector of the completion, as sketched in, e.g., Ref. [59], is expected to contain terms reading schematically as

$$\Delta\mathcal{L}_{\alpha^3 R^4}^{\text{SUSY, bos.}} \supset R^3 F_p^2, R^3 |F_p|^2, R^2 F_p^4, R^2 |F_p|^4, R F_p^6, R |F_p|^6. \quad (6)$$

The nonvanishing invariant tensor contractions among them clearly generate axion kinetic term corrections up to sextic order arising from the powers of $|F_p|^2$. Moreover, the possible invariants generating these higher-order axion kinetic terms may involve topological invariants of the compactification space arising from integrating over powers of curvature on the internal space. These topological invariants, like, e.g., the Euler characteristic, may lead to sizable numerical enhancements of the higher-order

axion kinetic terms, providing a rationale for their mass scales to scan a range of values relative to the Planck scale.

The higher-derivative axion kinetic term series inferred from the SUSY completion of the $\alpha^3 R^4$ terminates at a finite order of derivatives at this order in α' . String theory is expected to generate corrections beyond $\mathcal{O}(\alpha^3)$ in an infinite series. This is of course a string theory avatar of our strong coupling EFT argument. Hence, at higher orders in α' , there will potentially exist invariants involving powers of the p -form field strengths producing higher-derivative axion kinetic terms beyond the maximal order generated at $\mathcal{O}(\alpha^3)$.⁴ But in weak coupling, these terms will be small. The closed string sector higher-order α' -corrections appear after reduction to four dimensions suppressed by powers of the inverse compactification volume [59].

Hence, barring an appearance of numerically very large topological numbers governing these higher-order α' -corrections, the higher-derivative axion kinetic terms potentially produced by them will have volume suppressed small coefficients relative to the higher-derivative axion kinetic terms appearing at $\mathcal{O}(\alpha^3)$. In this sense, the series of higher-derivative axion kinetic terms with potentially sizable coefficients appearing via dimensional reduction from the ten-dimensional (10D) closed string sector will effectively terminate at sextic order. In other words, to get larger effects, one must approach the limits of the validity of the compactified theory, as expected from the generic EFT consideration.

Again, we stress that the above observations about (ir)relevance of higher-derivative terms are features of the weak coupling limit of the theory, well below the relevant cutoff of the inflationary EFT, and under the assumption that the Hilbert space of states is largely unaffected by the background evolution of fields and couplings. As we approach the limits of the inflationary EFT, by cranking up the field values and couplings, the irrelevant operators, including the higher-derivative ones, will become more influential. To account for those effects, we must be careful when comparing the higher-derivative axion kinetic terms arising from dimensional reduction of the 10D higher-derivative p -form field strength powers to the higher-derivative axion kinetic terms outlined in Ref. [10]. It is here where the origin of the low energy axions is important. The point is that simple “derivative accounting” may be misleading, which can be seen as follows. Consider a low energy EFT axion, which acquires its quadratic potential via mixing with the 4-form field strength in the 4D effective flux monodromy description of Ref. [41] and is a pseudoscalar magnetic dual of a perturbative p -form string axion, that comes from dimensional reduction. At two-derivative level, all the known string axion and brane monodromy inflation mechanisms can be dualized into this

4D effective 4-form description [60]. This procedure is useful since it makes the hidden gauge symmetries of the theory manifest, providing the tools to control the strong coupling regime. However, it also shows that once the dimensionally reduced p -form string axions acquire higher-derivative kinetic terms, it becomes quite nontrivial to match these to the description of the higher-derivative kinetic terms of the dual axion of the 4D effective 4-form theory, as encoded in couplings of the type $(A_3 - dB_2) \wedge \star F_4$ with B_2 being the 4D dual 2-form gauge potential describing the axion degree of freedom from the compactified string model. In a nutshell, dualization is a canonical transformation [43,61], and so in perturbation theory, the derivatives of the axion are mapped to the powers of the 3-form mass term and vice versa. This is simply the consequence of the fact that a canonical transformation exchanges generalized coordinates and momenta, $(q, p) \leftrightarrow (-P, Q)$, while preserving the commutation relations and the Hamiltonian [43,61]. The full “resummation” of the perturbative duality maps also “dresses” up the Hilbert space vacuum, very similarly to what happens with the BCS vacuum below the critical temperature, when the condensate forms. Thus, it is perfectly plausible that a theory with higher derivatives on one side may appear as a totally nonderivative theory on the other side.

A flavor of the nontrivial duality matching is already visible in the 4-form description of hybrid axion monodromy in Ref. [62], in which the nontrivial issues concerning the selection of the vacuum are noted. Here, we set such a full duality matching at higher-derivative order aside, given the uncertainties with the perturbative dimensionally reduced p -form string axion sector at higher derivatives. We do expect that upon performing the duality match, the finite order of the higher-derivative axion kinetic terms expected for a closed string axion at $\mathcal{O}(\alpha^3)$ will translate to a matching finite higher-derivative order of the kinetic terms for the dual 4D effective axion of the 4-form EFT, which suffices for our purposes. We should also note that even when the strong coupling effects induce large higher-derivative operators, there are still regimes where initial conditions for classical evolution allow flattened potentials to dominate, thus “deactivating” the higher-derivative terms [10]. This regime is also illustrated by our truncation of the derivative expansion. Obviously, this means there could be other branches of solutions which we ignore here.

IV. VARIATIONS FOR BICEP3

Having set up the stage for the EFT of double monodromy, with or without strong coupling effects included, and highlighted its relationship to the UV completions in models where inflatons are axions or brane positions, we can now leverage the universality of the 4D EFT to study the axion inflation dynamics at strong coupling. The homogeneous field configurations satisfy $16\pi^2 X_1/M^4 \gtrsim 1$ and $16\pi^2 V_{\text{eff}}/M^4 \gtrsim 1$. Truncating to the quartic time

⁴We thank Timo Weigand for discussions concerning this point.

derivative terms for simplicity, as outlined above, the slow-roll field equations are⁵

$$3M_{\text{pl}}^2 H^2 = V_{\text{eff}}, \quad 6H\dot{\phi}_1 \ddot{Z}X_1 = -4\pi M^2 m V'_{\text{eff}}. \quad (7)$$

There are evolutionary regimes for the fields depending on the relevance of the derivative terms relative to the potential. A discussion of options was given in Ref. [10]. A case of interest to us here is where the higher-derivative operators are both large in the EFT and are excited, contributing to the background during slow-roll inflation.⁶ In this case, the tensor power is suppressed thanks to both the flattened potential and the subluminal speed of sound of the perturbations, induced by the higher derivatives. An important additional consideration is that the higher-derivative terms induce nonlinearities which yield non-Gaussianities. The bounds on non-Gaussianities, $f_{\text{NL}} \lesssim \mathcal{O}(10)$ imply a *lower* bound on r .

To compute the perturbations on the background controlled by the slow-roll equations (7), we deploy the formalism of the inflaton EFT [63], ignoring the mixing with gravity. This approximation is good at energy scales $E \gg \sqrt{\epsilon}H$ and $c_s^2 \gg \epsilon$, which apply in our case. The spectrum of perturbations is almost scale invariant and has small non-Gaussianities, as observations require. In the gauge where the spatial metric is unperturbed, the field perturbation is $\phi_1(t, \vec{x}) = \varphi_0(t + \pi(t, \vec{x}))$, whereas the spatial curvature perturbation is $\mathcal{R} = -H\pi$. Expanding Eq. (3) up to third order, and keeping only the terms lowest in derivatives,

$$S = - \int dt d^3\vec{x} a^3 M_{\text{pl}}^2 \dot{H} \left[\frac{1}{c_s^2} \dot{\pi}^2 - \frac{(\partial_i \pi)^2}{a^2} + \left(\frac{1}{c_s^2} - 1 \right) \times \left(\dot{\pi}^3 + \frac{2}{3} c_3 \dot{\pi}^3 - \dot{\pi} \frac{(\partial_i \pi)^2}{a^2} \right) \right]. \quad (8)$$

Dropping the subscript 1 from here on, and using our monodromy EFT (3), the speed of sound is $c_s^2 = \partial_X \mathcal{K} / (\partial_X \mathcal{K} + 2X \partial_X^2 \mathcal{K})$, and $c_3(1/c_s^2 - 1) = 2X^2 \partial_X^3 \mathcal{K} / \partial_X \mathcal{K}$. So,

when $X > \frac{M^4}{16\pi^2}$, we find $c_s^2 \sim \frac{M^4}{32\pi^2 X} \frac{\mathcal{K}''}{\mathcal{K}'}$ and $c_3(1/c_s^2 - 1) = \frac{512\pi^4 X^2 \mathcal{K}'''}{M^8 \mathcal{K}'^2}$, or $c_3 = \frac{16\pi^2 X \mathcal{K}'''}{M^4 \mathcal{K}''}$. The exact details of the theory when $y = 16\pi^2 X / M^4 > 1$, which set the magnitude of \mathcal{K} and its derivatives, depend on the UV theory governing the large- y asymptotia.

As in weak coupling, the amplitude perturbation is controlled by horizon scale when $\lambda^{-1} \simeq H$. The Gaussian curvature perturbation is determined by folding this scale with the time translation breaking scale. In contrast to the weak coupling regime, where $\sqrt{\bar{\varphi}} = (2M_{\text{pl}}^2 \dot{H})^{1/4} = \epsilon_H^{1/4} \sqrt{2M_{\text{pl}} H} \gg H$, in the strong coupling regime with large derivative terms, one finds that this scale is $f_\pi^4 = 2M_{\text{pl}}^2 \dot{H} c_s$. Note, that by Eq. (3) in this regime, $M_{\text{pl}}^2 H^2 \simeq \frac{M^4}{16\pi^2}$. The Gaussian scalar power spectrum is $\Delta_{\mathcal{R}}^2 \propto (H/f_\pi)^2$.

The leading non-Gaussianities in this regime come from the three-point function. There are two operators in (8) which source them. However, since by naturalness and naive dimensional analysis arguments all the derivatives are comparable, $c_3 \simeq c_s^2 < 1$, and so the non-Gaussianities generated by the $\sim c_3$ term are subleading. Thus, the amplitude of the cubic non-Gaussianities reduces to a single narrow strip [10]. Using the perturbation potential

$$\langle \Phi_{\vec{k}_1} \Phi_{\vec{k}_2} \Phi_{\vec{k}_3} \rangle = (2\pi)^3 \delta_D(\vec{k}_1 + \vec{k}_2 + \vec{k}_3) \frac{6\Delta_\Phi^2}{(k_1 + k_2 + k_3)^3} \times [f_{\text{NL}}^{(1)} F_1(k_1, k_2, k_3) + f_{\text{NL}}^{(2)} F_2(k_1, k_2, k_3)], \quad (9)$$

we find that the F_1 and F_2 are induced by the $\dot{\pi}(\partial\pi)^2$ and $\dot{\pi}^3$ operators, respectively [55,64,65]. Explicitly, we define

$$K_1 = k_1 + k_2 + k_3, \quad K_2 = (k_1 k_2 + k_2 k_3 + k_3 k_1)^{1/2}, \quad K_3 = (k_1 k_2 k_3)^{1/3}, \quad (10)$$

in terms of which

$$F_1 = - \frac{9}{17} \frac{12K_3^6 - 4K_1 K_2^2 K_3^3 - 4K_1^4 K_2^2 + 11K_1^3 K_3^3 - 3K_1^4 K_2^2 + K_1^6}{K_3^9}, \quad F_2 = \frac{27}{k_1 k_2 k_3}. \quad (11)$$

⁵When solving numerically, we work with the full $K(X)$ function in Eq. (7) in the slow-roll approximation.

⁶As we explained above, it is possible that large higher-derivative operators are present in the effective action but that the initial conditions at the observable stage of inflation are such that these are subleading to the quadratic derivatives and remain so in slow roll. We ignore this here.

The term $\propto F_1$ describes equilateral non-Gaussianities, since the momentum dependence is such that it is maximized when all three momenta are equal, while the term $\propto F_2$ shows an important contribution also on flattened triangles. CMB analyses [64,65] are commonly done in terms of two templates, the equilateral one which is very similar to F_1 and an orthogonal one which is a linear combination of F_1 and F_2 . In terms of the Lagrangian parameters, the f_{NL} coefficients are

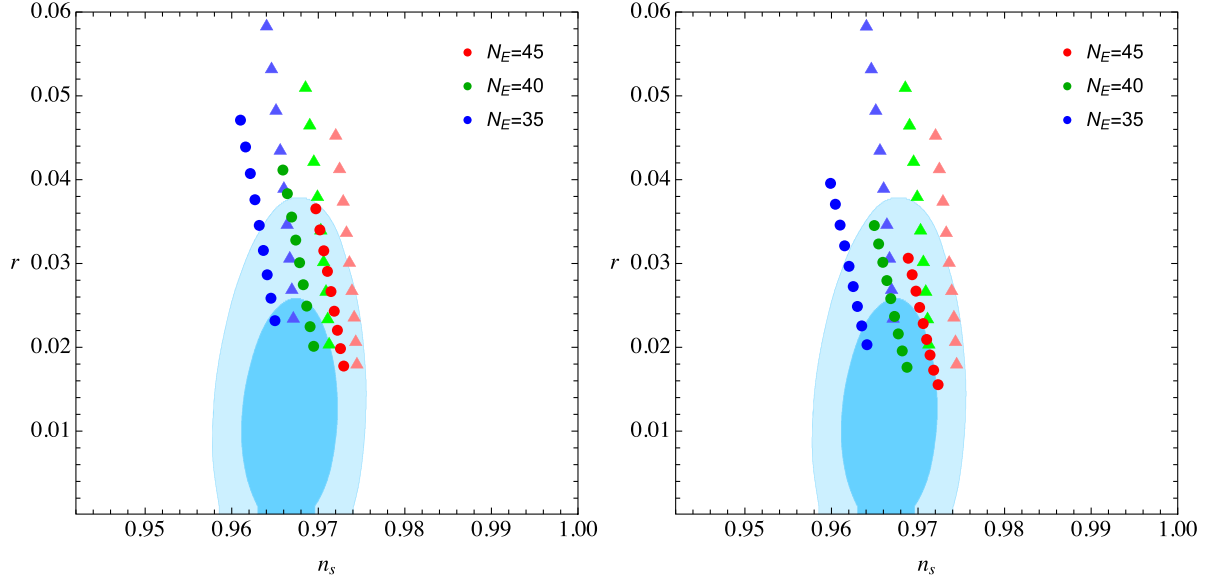


FIG. 2. Tensor-to-scalar ratio vs spectral index for double monodromy with quartic (left) and sextic (right) kinetic terms, compared to the data of Ref. [4]. In the left panel, $K(X) = X + X^2/M_4^4$, with $M_4 = 0.05$, while in the right panel, $K(X) = X + X^3/M_6^8$, fixing $M_6 = 0.05$. We take $\mu_1 = 0.01$ and vary $0.1 \leq p_1 \leq 0.5$. The triangles depict the quadratic kinetic term case ($c_s = 1$), while dots are the predictions for the higher derivatives. A finite M_4 or M_6 will give a redder spectrum [67] and a lower r .

$$f_{\text{NL}}^{(1)} = -\frac{85}{324} \left(\frac{1}{c_s^2} - 1 \right), \quad f_{\text{NL}}^{(2)} = -\frac{10}{243} (1 - c_s^2) \left(\frac{3}{2} + c_3 \right). \quad (12)$$

For our quartic and sextic models, c_3 in Eq. (12) is -3 and -4 , respectively, so $f_{\text{NL}}^{(2)}$ is very small with respect to $f_{\text{NL}}^{(1)}$, by a factor $1/c_s^2$; for DBI, $f_{\text{NL}}^{(1)} = -(17/4)f_{\text{NL}}^{(2)}$, and they have the

same dependence on c_s^2 . For definiteness, we show $f_{\text{NL}}^{(1)}$ in Figs. 3 and 4. The experiments are already constraining the phase space of even the strongly coupled theory. From Planck [66], marginalizing over c_3 , one gets the bound $c_s \gtrsim 0.21$. This yields $X \lesssim M^4/10$. Thus, the theory should be in strong coupling to prevent too large r , but it cannot be arbitrarily strongly coupled to satisfy the bound on non-Gaussianities. Hence, the tensor power cannot be arbitrarily weak.

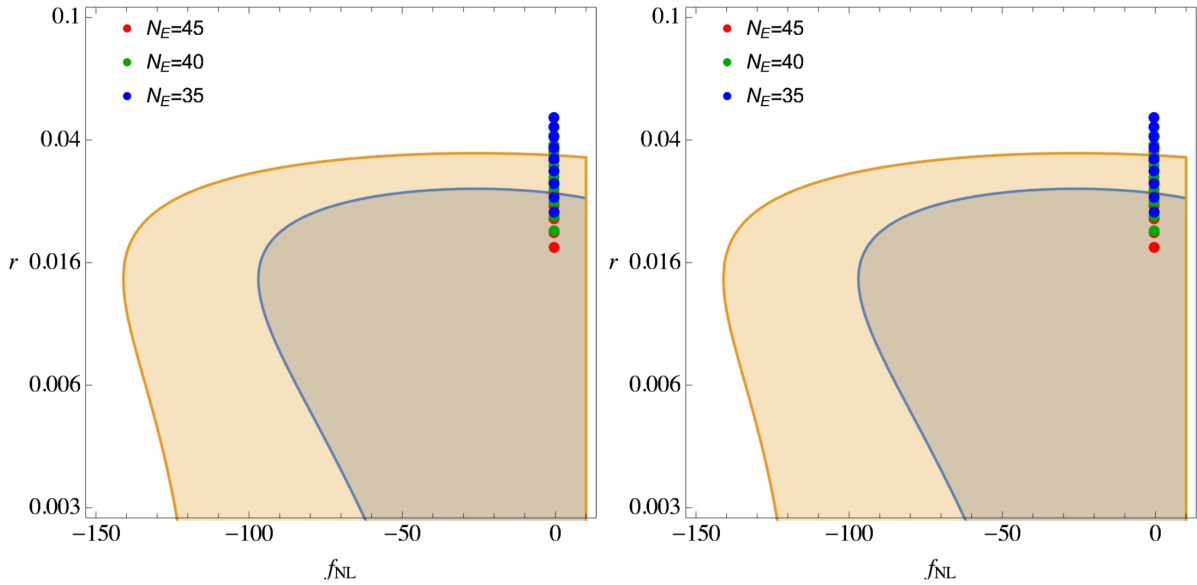


FIG. 3. Tensor-to-scalar ratio r vs equilateral non-Gaussianity f_{NL} for double monodromy with quartic (left) and sextic (right) kinetic terms. The parameters are the same as in Fig. 2. Because of the lower bound on c_s in either model ($c_s^2 > 1/3$ for quartic, $c_s^2 > 1/5$ for sextic), the non-Gaussianity is very small.

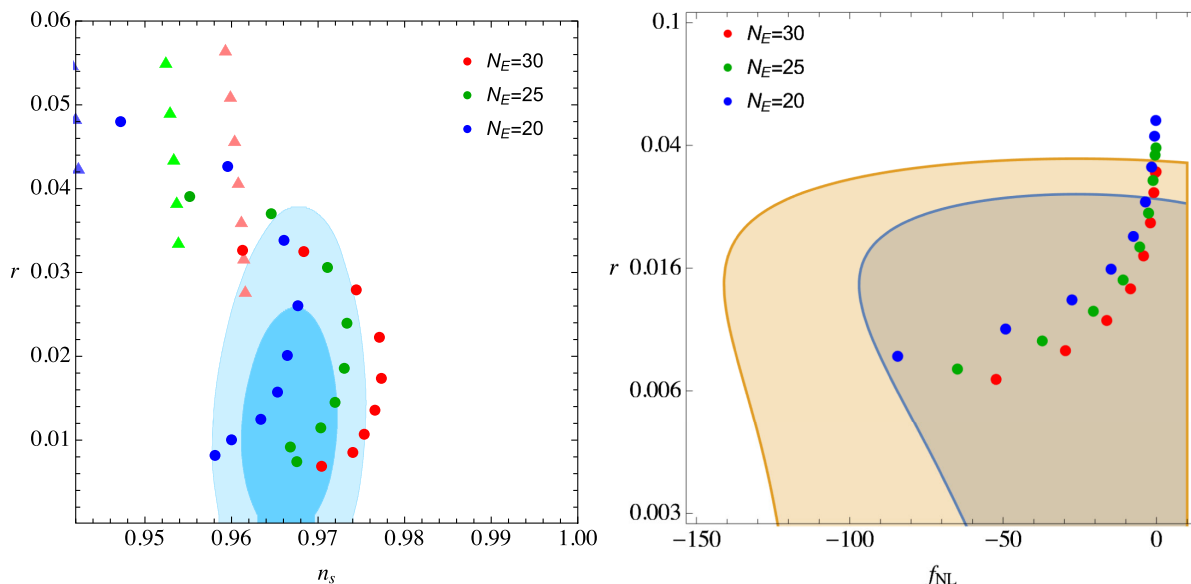


FIG. 4. Tensor-to-scalar ratio r vs spectral index n_s (left) and r vs equilateral non-Gaussianity f_{NL} (right) for double monodromy with DBI kinetic terms. We take $\mu_1 = 0.01$ for the potential, vary $0.1 \leq p \leq 0.5$, and fix $M = 0.23$. In the left panel, the triangles denote solutions with the canonical kinetic term, while the dots are solutions for the DBI kinetic term. We note that, since c_s is not bounded from below, r can be much lower in the DBI model with respect to quartic and sextic kinetic terms. Equilateral non-Gaussianity shows the expected inverse correlation with r , but it is within the current experimental bounds.

In Figs. 2 and 3, we show the predictions for the observables r , n_s , and f_{NL} , for our potential Eq. (4) and kinetic terms with either quartic or sextic higher-derivative terms, in a regime in which these higher-derivative corrections are important. In Fig. 4, we show the predictions for our double monodromy potential with a DBI kinetic term, $K(X) = M^4(1 - \sqrt{1 - 2X/M^4})$, which produces an infinite series of higher-derivative corrections. In comparing to the results of Ref. [67], it is important to note that there the higher derivatives arise from integrating out a heavy scalar generating an infinite series of higher-derivative operators. In the particular example displayed in Fig. 5 in Ref. [67], this infinite series resums into a cosine potential in V and a cosine dependence in c_s . This produces the strong reddening of n_s with decreasing c_s visible in the blue down-left curving band of Fig. 5 of Ref. [67]. In our first example, we only keep a quartic and/or sextic higher derivatives in the kinetic term; hence, the reddening of n_s remains much milder for our case. Moreover, with decreasing c_s and thus increasing effects of the higher-derivative operators, we get pushed out of the quadratic part of the scalar potential onto the flatter-monomial “wings,” which causes a blueshift of n_s , partially offsetting the reddening effects of the higher derivatives themselves. Meanwhile, in the example of Fig. 5 in Ref. [67], decreasing c_s and thus increasing effects of the higher derivatives pushes one toward the hilltop of a cosine potential which by itself causes additional reddening of n_s .

For the quartic and sextic kinetic terms, we observe that for powers $p \gtrsim 0.1$, we get small non-Gaussianities, tensor-to-scalar ratio in the range $r \gtrsim 0.015$, and $0.96 \lesssim n_s \lesssim 0.97$ for the first stage of inflation which ends after 35–45 e -folds. For the DBI kinetic term, we get $r \gtrsim 0.006$ and larger f_{NL} for the first stage of inflation ending after 20–30 e -folds. Summarizing, with nonstandard kinetic terms, the model remains a fully viable fit of the sky at the CMB scales, but with predictions in the reach of the near-future cosmological observations, such as the next installment of BICEP or LiteBIRD. This makes our natural monodromy models an excellent benchmark for future observations. Further, the mechanism of nonperturbative generation of chiral tensors, using vector tachyon instability [1,68,69], which we review below in this new context, remains operational and can yield additional gravity wave signals at shorter scales.

V. FÜR LISA, AN ENCORE, WITH OTHER INSTRUMENTS, TOO

We noted in Ref. [1] that axionlike inflatons often couple to $U(1)$ gauge fields via the standard dimension-5 operators $\propto \phi_1 F_{\mu\nu} \tilde{F}^{\mu\nu}/2$. A simple example is to start with a 4-form field strength in 11D supergravity, with Chern-Simons self-couplings and dimensionally reduce it on some toroidal compactification. Ignoring the moduli fields, the resulting 4D effective action will include light axions coupled to dark $U(1)$ s since

$$\begin{aligned}
& -F_{abcd}^2 + \epsilon_{a_1 \dots a_{11}} A^{a_1 \dots} F^{a_4 \dots} F^{a_8 \dots a_{11}} \\
& \ni -F_{\mu\nu\lambda\sigma}^2 - (\partial\phi_1)^2 - \mu\phi_1 \epsilon_{\mu\nu\lambda\sigma} F^{\mu\nu\lambda\sigma} \\
& - \sum_k F_{\mu\nu(k)}^2 - \frac{\phi_1}{f_\phi} \sum_{k,l} \epsilon_{\mu\nu\lambda\sigma} F^{\mu\nu(k)} F^{\lambda\sigma(l)}. \quad (13)
\end{aligned}$$

Here, the first line lists the 4-form-axion sector, which thanks to the monodromy coupling is massive but light, and the second describes the mixing of the axion with dark $U(1)$ s. If for simplicity we take only one coupling to be nonzero, we can model it with the canonically normalized 4D dimension-5 operator

$$\mathcal{L}_{\text{int}} = -\sqrt{-g} \frac{\phi_1}{4f_\phi} F_{\mu\nu} \tilde{F}^{\mu\nu}, \quad (14)$$

where f_ϕ is sub-Planckian. This scale is generically $\simeq M_{\text{GUT}}$ (see, e.g., Refs. [47,48]). A rolling axion triggers the tachyonic instability of one circular polarization of the gauge field [70], whose exponential production both backreacts on the inflaton and produces scalar and tensor perturbations [68,69]. Details of the backreaction were examined in Refs. [71,72], and a very comprehensive analysis of these effects was provided recently in Ref. [73], with the results of the nonperturbative treatment recently cross-verified in Ref. [74] using a completely different gradient expansion formalism down to numerically identical predictions of the GW signal including resonance-induced peaked fine structure. The details of the dynamics are given in Refs. [1,73], and we will not repeat them here. We should mention the other works which have recently explored bumpy early Universe dynamics to generate relic gravity waves [75–81].

We imagine this axion to be the inflaton dominating the first stage of inflation in the double monodromy inflation of the previous section, which in addition to the simple quadratic potential [given in the dual 4-form frame by the first line of Eq. (13)] also includes additional corrections, that combine into the potential (1) and the higher-derivative operators (2). Thus, early on during the first stage of inflation, the dynamics described in the previous section yields a suppressed tensor-to-scalar ratio and weak non-Gaussianities, while matching the scalar CMB spectrum. By the end of this stage, however, the inflaton drops out of the strong coupling, and inflation continues for a few more e -folds in weak coupling. This last epoch of the first stage of inflation is described by the terms of Eq. (13). Hence, the analysis of sub-CMB gravity wave generation of Ref. [1], describing how the tachyonic instability in the dark $U(1)$ is triggered by (14), goes through unabated. Hence, a $U(1)$ chirality is cranked up, and it in turn sources chiral gravity waves. The amplification is quite efficient, although it is bounded by inflaton kinetic energy and scale of the first stage of inflation near its end. Assuming that the potential (4) remains valid all the way to the end of the weakly

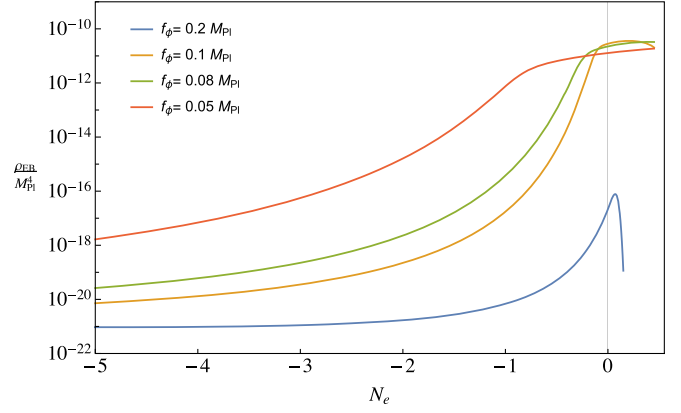


FIG. 5. Evolution at the end of the first inflationary stage of the energy density in gauge fields. We denote by N_e the number of e -folds before the end of the first stage of inflation, and we normalize the energy density to M_{Pl}^4 . The parameters of the potential are fixed for convenience to $M_1^4 = 2 \times 10^{-9} M_{\text{Pl}}^4$, $\mu_1 = M_{\text{Pl}}$, $p = 0.2$; at the CMB scales, they lead to similar results as $\mu_1 = 0.1 M_{\text{Pl}}$, which fit CMB perfectly. We show results for different couplings f_ϕ as shown in the legend. The vertical line denotes the end of inflation, and the solutions we show are not completely reliable there. Note that the contributions of the vector field are very small until the very end of inflation, when ϕ_1 moves the fastest. As a result, the $U(1)$ production does not affect CMB significantly.

coupled epoch of the first stage of inflation, the energy density transferred to the tachyonic chirality of the dark $U(1)$ can be calculated numerically, as presented in Fig. 5.

We should stress that some of these modes will reenter the horizon during the intermediate matter-dominated stage, interrupting the two stages of inflation. Hence, they would dilute by expansion during that epoch. However, as long as the interruption is short, the dilution is weak. We can estimate it as follows: for subhorizon wavelength modes, the amplitude goes as $1/\lambda \sim 1/a$, where a is the scale factor. Since these modes are harmonic oscillators, their power, by the virial theorem, is given by the square of frequency \times the amplitude. Hence, the suppression factor will be at most $(a_1/a_2)^4$, where a_1 is the scale factor at the end of stage 1 of inflation and a_2 is the scale factor at the mode refreezing after the start of the next stage inflation. This factor is largest for the shortest wavelength mode at the end of stage 1, for which $k/a_1 \sim H_1$. Because the mode freeze-out yields $k/a_2 \simeq H_2$, this yields $a_1/a_2 \lesssim H_2/H_1$, and so for a short interruption, the power suppression would be no more than a factor of 100 to 1000, which is why we ignored it here. A more precise calculation is warranted here, both for the computation of the proper signal benchmarks and, crucially, since this also evades violations of the big bang nucleosynthesis (BBN) bound on gravity waves, $\Omega_{\text{GW}} h^2 \lesssim 10^{-6}$ [82]. For this reason, we sketch these uncertainties in the prediction, plotting a gray band, spanning 2 orders of magnitude, around the idealized prediction of the power emitted in GWs in Figs. 6 and 7.

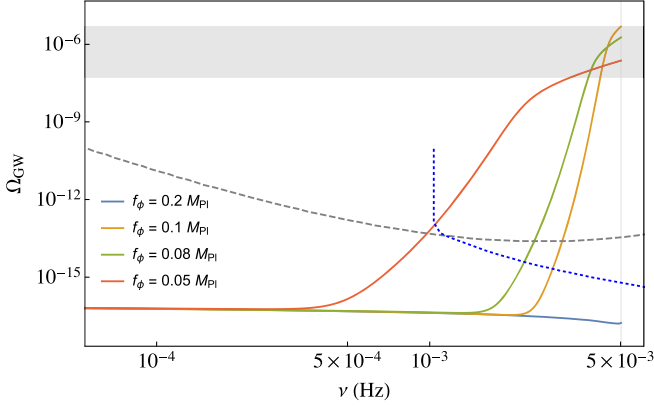


FIG. 6. Abundance of gravitational waves as a function of frequency, setting $N_{\text{CMB}} = 35$. The dashed gray line is the sensitivity of LISA [83], and the dotted blue line is the sensitivity of Big Bang Observer (BBO) [84]. Again, we use $M_1^4 = 2 \times 10^{-9} M_{\text{Pl}}$, $\mu_1 = M_{\text{Pl}}$, $p = 0.2$ for convenience, and as before scan f_ϕ as shown in the legend. The vertical line again designates the end of inflation, beyond which a different approximation is needed. We plot maximal power here, ignoring the suppression during the interruption. The gray band outlines the uncertainties due to this suppression, which when accounted for evade violations of the BBN bound on gravity waves.

In turn, the tachyonic dark $U(1)$ modes source the stochastic gravity waves which are chiral, with the total abundance which can be estimated by [86]

$$\Omega_{\text{GW}} \equiv \frac{\Omega_{r,0}}{24} \Delta_T^2 \simeq \frac{\Omega_{r,0}}{12} \left(\frac{H}{\pi M_{\text{Pl}}} \right)^2 \times \left(1 + 4.3 \times 10^{-7} \frac{H^2}{M_{\text{Pl}}^2 \xi^6} e^{4\pi\xi} \right), \quad (15)$$

where $\Omega_{r,0} = 8.6 \times 10^{-5}$ is the radiation abundance today, $\xi = \frac{\dot{\phi}}{2Hf_\phi}$, and the terms are evaluated at horizon crossing. The equation is valid for $\xi \gtrsim 3$. This is the sum of the two polarization of gravitational waves: the 1 term in the parentheses arises due to the usual metric fluctuations in de Sitter space and includes the contributions from both graviton helicities. The second term in parentheses, involving the exponential amplification, receives contribution only from the helicity sourced by the ‘‘tachyonic’’ gauge field source, as evidenced by its dependence on ξ . By mode orthogonality in the linearized limit, the other graviton helicity is not enhanced.

It is clear that a favorable realization of the scales can enhance the primordial GW spectrum dramatically. To fix the physical wavelength of these modes, which allows us to see by which instrument they might be searched for, and what their amplitude at the relevant wavelength is, we can rewrite Ω_{GW} as a function of the frequency observed at the present time. Since the comoving frequency is $\nu = k/(2\pi)$, the frequency of the modes in terms of the number of e -folds before the end of inflation is given by

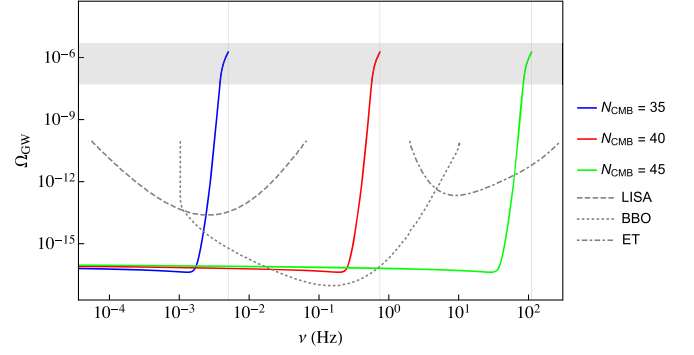


FIG. 7. Abundance of gravitational waves as a function of frequency, setting for different $N_{\text{CMB}} = 35, 40, 45$. We show the predicted bounds as a function of frequency for LISA [83], Big Bang Observer (BBO) [84], and Einstein Telescope (ET) [85]. We use $M_1^4 = 2 \times 10^{-9} M_{\text{Pl}}$, $\mu_1 = M_{\text{Pl}}$, $p = 0.2$, and $f_\phi = 0.08$. If n_s is bluer, for monodromy models, this means longer (first stage of) inflation. If at the end of this stage chiral tensors are generated, their frequency will be higher. The vertical line designates the end of inflation for each curve, beyond which a different approximation is needed. Again, the gray band outlines the uncertainties in the prediction of the power due to the suppression at the interruption between the stages of roller-coaster inflation.

$$N = N_{\text{CMB}} + \ln \frac{k_{\text{CMB}}}{0.002 \text{ Mpc}^{-1}} - 44.9 - \ln \frac{\nu}{10^2 \text{ Hz}}, \quad (16)$$

where $k_{\text{CMB}} = 0.002 \text{ Mpc}^{-1}$ is the CMB pivot scale and N_{CMB} is the number of e -folds before the end of the first stage of inflation where the CMB scales froze out. With this, we can regraph the results of Fig. 5 in terms of the new independent variable ν and the GW amplitude Ω_{GW} . The results are presented in Fig. 6. Again, the approximations which we employ are not completely reliable beyond the end of inflation, and noted above and in Ref. [1]. However, they remain a good indicator of the signal’s power.

Of course, as we have seen from the previous discussion, and showed manifestly in, e.g., Fig. 2, we can automatically satisfy the CMB bounds on n_s and r for a range of N_{CMB} . This means that there are degeneracies in the evolution allowing for a good fit the CMB for a range of models, with different values of the pivot point N_{CMB} —i.e., with the ‘‘CMB epoch’’ of multistage inflation of varying duration. Therefore, we find it interesting to fix f_ϕ and plot $\Omega_{\text{GW}}(\nu)$ for different values of N_{CMB} , which generates a horizontal shift of the curves of Fig. 6. This plot is in Fig. 7, from which it is apparent that several experiments in the near future can explore the parameter space of our model. What is more is that such a mechanism might occur at the end of every accelerated stage of roller coaster, due to the inflatons being axionlike and possibly coupling to many different dark $U(1)$ s, thus producing what we might dub a ‘‘characteristic spectrum’’ of roller-coaster models. If so, then each spike, a different range of scales, might be simultaneously probed by one of the planned instruments.

The bottom line is that these modes may very well be out there for the GW instruments to discover. Depending on the specifics of the earliest stage of inflation and its duration, their wavelength might be in the sweet spot of LISA [83] or DECIGO/BBO [84] or, if the wavelength is longer (and the earlier stage of inflation shorter), SKA or NANOgrav (for a recent study of the measurement of the spectrum of primordial gravitational waves, see Ref. [87]). In either case, combining this with the bounds on r at the CMB scales makes our double-coaster, and more generally multistage roller coaster, extremely predictive and easy to confirm.

VI. CONCLUSION

We have updated here our earlier model of double monodromy inflation with the inclusion of the general strong coupling-induced irrelevant operators, which lead to additional suppression of the tensor-to-scalar ratio in inflation. As a result, the predictions of the model, which involves an early stage of inflation which is interrupted by the first inflaton decay 25–40 e -folds after the beginning, are fully consistent with the most recent BICEP/Keck bounds. The observables are $0.006 \lesssim r \lesssim 0.035$ with $0.96 \lesssim n_s \lesssim 0.97$ with $f_{\text{NL}} \lesssim \mathcal{O}(10)$. This makes the models very predictive since they can be constrained—and possibly confirmed and ruled out—by the very near-future observations. In addition, the first inflaton could couple to a hidden sector $U(1)$ and lead to an enhanced production of vectors near the end of the first stage of inflation. These vectors in turn would source tensors at shorter wavelengths, leading to additional signatures of the model that would correlate with the signatures in the CMB.

In closing, we should finally mention that at this point, however, it may still be premature to take the $n_s - r$ bounds as very strong obstructions to inflationary models. Namely, although the bounds on r are strong, the correlation of n_s and r might be weaker than it seems. We believe the situation warrants a warning of sorts since the $n_s - r$ correlation is commonly used to assess the likelihood of popular inflationary models (nice reviews of the observational constraints on theoretical models can be found in, e.g., Refs. [2,3]). For example, one commonly encounters the “potato plots” such as in Fig. 5 in Ref. [4] or Fig. 4 in the subsequent paper [88] as well as our own Figs. 2–4, which one may take to suggest there is very small remaining parameter space for inflationary models to “squeeze in.” Such reasoning might be too quick, since there is another interesting possibility that can open up the space in the $n_s - r$ plane, which is quite curious although it might seem somewhat extreme.

The issue is that in all the figures plotting r versus n_s which we have shown so far we have relied on the constraints on n_s based on the CMB data analysis *assuming* the Λ CDM model of the late Universe. However, for some years now, the measurements of the Hubble parameter

using standard candles [15,16,19,24] have shown discrepancy with the value of H_0 determined by Planck experiment, which is based on fitting the CMB data to the late Λ CDM cosmology [89]. To resolve the Hubble tension, many models have been proposed to date (for reviews, see Refs. [22,23]). Among the most successful models are the so-called early dark energy proposals, which involve additional degrees of freedom before recombination [20,21,90,91]. Analyzing the CMB data in terms of these new models, a common feature is that the spectral index is bluer with respect to the Λ CDM value (see Refs. [17,92–95]). If it indeed turns out that the Hubble tension is real, and the most recent examinations indicate support for this option, assessing the discrepancy to be at 5σ at this time [24], the shift of n_s will have very important implications for inflationary model constraints.

We illustrate this in Fig. 8, in which we plot the contours obtained from the Λ CDM model and the one we infer from the constraints on n_s in the so-called new early dark energy (NEDE) model, presented in Refs. [20,21]. This plot clearly shows how—all of a sudden—flattened monodromy models, with a long stage of inflation, and the power law behavior of, for example, $\sim \phi^{1/2}$ at large ϕ , which were supposedly excluded by having too large an n_s , may end up being better candidates than, for example, the Starobinsky R^2 . Of course, it is too soon to claim this. But until the H_0

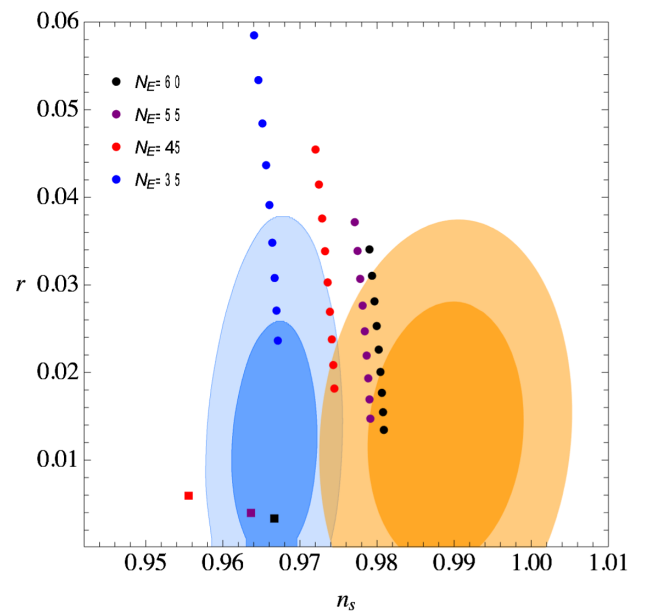


FIG. 8. Tensor-to-scalar ratio r vs spectral index n_s , for the Λ CDM model (blue) and for the NEDE model (gold). To get the NEDE model constraint, we approximate the Λ CDM contour as a bivariate Gaussian and substitute the mean and error on n_s by the ones gotten in the NEDE model. This approximate procedure reproduces well a full analysis [93]. The round dots are predictions of potentials (1) with $0.1 \leq p_1 \leq 0.5$, as before. The square dots are the predictions of the Starobinsky R^2 inflation [96].

tension is resolved, it may also be too soon to claim the opposite. The point is that we need to resolve the issues which arose in the late Universe cosmology before we can get into the precision data confirming or ruling out inflationary models. With the ever better quality of data and an array of planned searches and tests in the very near future, this seems to be within reach.

We therefore remain quite curious about what the future observations may yield.

ACKNOWLEDGMENTS

We would like to thank V. Domcke, P. Graham, R. Kallosh, A. Lawrence, A. Linde, F. Niedermann, E. Silverstein, M. Sloth, and T. Weigand for many very useful discussions. N.K. is supported in part by the DOE Grant No. DE-SC0009999. A.W. is supported by the ERC Consolidator Grant STRINGFLATION under the HORIZON 2020 Grant No. 647995.

-
- [1] G. D’Amico, N. Kaloper, and A. Westphal, Double monodromy inflation: A gravity waves factory for CMB-S4, LiteBIRD and LISA, *Phys. Rev. D* **104**, L081302 (2021).
 - [2] E. Silverstein, TASI lectures on cosmological observables and string theory, in *Theoretical Advanced Study Institute in Elementary Particle Physics: New Frontiers in Fields and Strings* (World Scientific, Singapore, 2017), pp. 545–606.
 - [3] R. Kallosh and A. Linde, BICEP/Keck and cosmological attractors, *J. Cosmol. Astropart. Phys.* **12** (2021) 008.
 - [4] P. A. R. Ade *et al.* (BICEP, Keck Collaborations), Improved Constraints on Primordial Gravitational Waves using Planck, WMAP, and BICEP/Keck Observations through the 2018 Observing Season, *Phys. Rev. Lett.* **127**, 151301 (2021).
 - [5] G. D’Amico and N. Kaloper, Rollercoaster cosmology, *J. Cosmol. Astropart. Phys.* **08** (2021) 058.
 - [6] L. McAllister, E. Silverstein, A. Westphal, and T. Wrase, The powers of monodromy, *J. High Energy Phys.* **09** (2014) 123.
 - [7] X. Dong, B. Horn, E. Silverstein, and A. Westphal, Simple exercises to flatten your potential, *Phys. Rev. D* **84**, 026011 (2011).
 - [8] N. Kaloper, A. Lawrence, and L. Sorbo, An ignoble approach to large field inflation, *J. Cosmol. Astropart. Phys.* **03** (2011) 023.
 - [9] S. Dubovsky, A. Lawrence, and M. M. Roberts, Axion monodromy in a model of holographic gluodynamics, *J. High Energy Phys.* **02** (2012) 053.
 - [10] G. D’Amico, N. Kaloper, and A. Lawrence, Monodromy Inflation in the Strong Coupling Regime of the Effective Field Theory, *Phys. Rev. Lett.* **121**, 091301 (2018).
 - [11] N. Kaloper and A. R. Liddle, Dynamics and perturbations in assisted chaotic inflation, *Phys. Rev. D* **61**, 123513 (2000).
 - [12] S. A. Kim and A. R. Liddle, Nflation: Multi-field inflationary dynamics and perturbations, *Phys. Rev. D* **74**, 023513 (2006).
 - [13] D. Wenren, Tilt and tensor-to-scalar ratio in multifield monodromy inflation, [arXiv:1405.1411](https://arxiv.org/abs/1405.1411).
 - [14] S. Dimopoulos and S. D. Thomas, Discretuum versus continuum dark energy, *Phys. Lett. B* **573**, 13 (2003).
 - [15] J. L. Bernal, L. Verde, and A. G. Riess, The trouble with H_0 , *J. Cosmol. Astropart. Phys.* **10** (2016) 019.
 - [16] L. Verde, T. Treu, and A. G. Riess, Tensions between the Early and the Late Universe, *Nat. Astron.* **3**, 891 (2019).
 - [17] E. Di Valentino, A. Melchiorri, Y. Fantaye, and A. Heavens, Bayesian evidence against the Harrison-Zel’dovich spectrum in tensions with cosmological data sets, *Phys. Rev. D* **98**, 063508 (2018).
 - [18] V. Poulin, T. L. Smith, T. Karwal, and M. Kamionkowski, Early Dark Energy can Resolve The Hubble Tension, *Phys. Rev. Lett.* **122**, 221301 (2019).
 - [19] W. L. Freedman *et al.*, The Carnegie-Chicago Hubble Program. VIII. An independent determination of the Hubble constant based on the tip of the Red Giant Branch, *Astrophys. J.* **882**, 34 (2019).
 - [20] F. Niedermann and M. S. Sloth, New early dark energy, *Phys. Rev. D* **103**, L041303 (2021).
 - [21] F. Niedermann and M. S. Sloth, Resolving the Hubble tension with new early dark energy, *Phys. Rev. D* **102**, 063527 (2020).
 - [22] E. Di Valentino, O. Mena, S. Pan, L. Visinelli, W. Yang, A. Melchiorri, D. F. Mota, A. G. Riess, and J. Silk, In the realm of the Hubble tension—a review of solutions, *Classical Quantum Gravity* **38**, 153001 (2021).
 - [23] N. Schöneberg, G. Franco Abellán, A. Pérez Sánchez, S. J. Witte, V. Poulin, and J. Lesgourgues, The H_0 Olympics: A fair ranking of proposed models, [arXiv:2107.10291](https://arxiv.org/abs/2107.10291).
 - [24] A. G. Riess *et al.*, A comprehensive measurement of the local value of the Hubble constant with 1 km/s/Mpc uncertainty from the Hubble space telescope and the SH0ES team, [arXiv:2112.04510](https://arxiv.org/abs/2112.04510).
 - [25] A. N. Lasenby and M. E. Jones, Using the cosmic microwave background to constrain H_0 , in *The Extragalactic Distance Scale, Proceedings of the ST Sci May Symposium* edited by M. Livio, M. Donahue, and N. Panagia (Cambridge University Press, Baltimore, MD, 1996), p. 76.
 - [26] W. H. Kinney, How to fool cosmic microwave background parameter estimation, *Phys. Rev. D* **63**, 043001 (2001).
 - [27] V. F. Mukhanov, CMB-slow, or how to estimate cosmological parameters by hand, *Int. J. Theor. Phys.* **43**, 623 (2004).
 - [28] R. E. Keeley, A. Shafieloo, D. K. Hazra, and T. Souradeep, Inflation wars: A new hope, *J. Cosmol. Astropart. Phys.* **09** (2020) 055.
 - [29] L. A. Kofman, A. D. Linde, and A. A. Starobinsky, Inflationary universe generated by the combined action of a scalar field and gravitational vacuum polarization, *Phys. Lett.* **157B**, 361 (1985).

- [30] L. A. Kofman and A. D. Linde, Generation of density perturbations in the inflationary cosmology, *Nucl. Phys.* **B282**, 555 (1987).
- [31] J. A. Adams, G. G. Ross, and S. Sarkar, Multiple inflation, *Nucl. Phys.* **B503**, 405 (1997).
- [32] A. A. Starobinsky, Multicomponent de Sitter (Inflationary) stages and the generation of perturbations, *JETP Lett.* **42**, 152 (1985), <https://inspirehep.net/literature/229378>.
- [33] D. Polarski and A. A. Starobinsky, Spectra of perturbations produced by double inflation with an intermediate matter dominated stage, *Nucl. Phys.* **B385**, 623 (1992).
- [34] P. Peter, D. Polarski, and A. A. Starobinsky, Confrontation of double inflationary models with observations, *Phys. Rev. D* **50**, 4827 (1994).
- [35] M. Cicoli, S. Downes, B. Dutta, F. G. Pedro, and A. Westphal, Just enough inflation: Power spectrum modifications at large scales, *J. Cosmol. Astropart. Phys.* **12** (2014) 030.
- [36] Z. Zhou, J. Jiang, Y.-F. Cai, M. Sasaki, and S. Pi, Primordial black holes and gravitational waves from resonant amplification during inflation, *Phys. Rev. D* **102**, 103527 (2020).
- [37] G. Tasinato, An analytic approach to non-slow-roll inflation, *Phys. Rev. D* **103**, 023535 (2021).
- [38] M. Braglia, D. K. Hazra, F. Finelli, G. F. Smoot, L. Sriramkumar, and A. A. Starobinsky, Generating PBHs and small-scale GWs in two-field models of inflation, *J. Cosmol. Astropart. Phys.* **08** (2020) 001.
- [39] E. Silverstein and A. Westphal, Monodromy in the CMB: Gravity waves and string inflation, *Phys. Rev. D* **78**, 106003 (2008).
- [40] L. McAllister, E. Silverstein, and A. Westphal, Gravity waves and linear inflation from axion monodromy, *Phys. Rev. D* **82**, 046003 (2010).
- [41] N. Kaloper and L. Sorbo, A Natural Framework for Chaotic Inflation, *Phys. Rev. Lett.* **102**, 121301 (2009).
- [42] R. Flauger, L. McAllister, E. Pajer, A. Westphal, and G. Xu, Oscillations in the CMB from axion monodromy inflation, *J. Cosmol. Astropart. Phys.* **06** (2010) 009.
- [43] N. Kaloper and A. Lawrence, London equation for monodromy inflation, *Phys. Rev. D* **95**, 063526 (2017).
- [44] A. R. Liddle, A. Mazumdar, and F. E. Schunck, Assisted inflation, *Phys. Rev. D* **58**, 061301 (1998).
- [45] P. Kanti and K. A. Olive, On the realization of assisted inflation, *Phys. Rev. D* **60**, 043502 (1999).
- [46] S. Dimopoulos, S. Kachru, J. McGreevy, and J. G. Wacker, N-flation, *J. Cosmol. Astropart. Phys.* **08** (2008) 003.
- [47] T. Banks, M. Dine, P. J. Fox, and E. Gorbatov, On the possibility of large axion decay constants, *J. Cosmol. Astropart. Phys.* **06** (2003) 001.
- [48] P. Svrcek and E. Witten, Axions in string theory, *J. High Energy Phys.* **06** (2006) 051.
- [49] M. Dias, J. Frazer, and A. Westphal, Inflation as an Information Bottleneck—A strategy for identifying universality classes and making robust predictions, *J. High Energy Phys.* **05** (2019) 065.
- [50] C. Armendariz-Picon, T. Damour, and V. F. Mukhanov, k-inflation, *Phys. Lett. B* **458**, 209 (1999).
- [51] J. Garriga and V. F. Mukhanov, Perturbations in k-inflation, *Phys. Lett. B* **458**, 219 (1999).
- [52] Y. Nomura, T. Watari, and M. Yamazaki, Pure natural inflation, *Phys. Lett. B* **776**, 227 (2018).
- [53] N. Kaloper and A. Lawrence, Natural chaotic inflation and ultraviolet sensitivity, *Phys. Rev. D* **90**, 023506 (2014).
- [54] A. Gruzinov, Consistency relation for single scalar inflation, *Phys. Rev. D* **71**, 027301 (2005).
- [55] X. Chen, M.-x. Huang, S. Kachru, and G. Shiu, Observational signatures and non-Gaussianities of general single field inflation, *J. Cosmol. Astropart. Phys.* **01** (2007) 002.
- [56] A. Hebecker, S. C. Kraus, and L. T. Witkowski, D7-brane chaotic inflation, *Phys. Lett. B* **737**, 16 (2014).
- [57] H. Jockers and J. Louis, The effective action of D7-branes in $N = 1$ Calabi-Yau orientifolds, *Nucl. Phys.* **B705**, 167 (2005).
- [58] K. Becker, M. Becker, M. Haack, and J. Louis, Supersymmetry breaking and alpha-prime corrections to flux induced potentials, *J. High Energy Phys.* **06** (2002) 060.
- [59] J. P. Conlon, F. Quevedo, and K. Suruliz, Large-volume flux compactifications: Moduli spectrum and D3/D7 soft supersymmetry breaking, *J. High Energy Phys.* **08** (2005) 007.
- [60] F. Marchesano, G. Shiu, and A. M. Uranga, F-term axion monodromy inflation, *J. High Energy Phys.* **09** (2014) 184.
- [61] G. Dvali, Three-form gauging of axion symmetries and gravity, [arXiv:hep-th/0507215](https://arxiv.org/abs/hep-th/0507215).
- [62] N. Kaloper, M. König, A. Lawrence, and J. H. Scargill, On hybrid monodromy inflation (Hic Sunt Dracones), *J. Cosmol. Astropart. Phys.* **03** (2021) 024.
- [63] C. Cheung, P. Creminelli, A. L. Fitzpatrick, J. Kaplan, and L. Senatore, The effective field theory of inflation, *J. High Energy Phys.* **03** (2008) 014.
- [64] L. Senatore, K. M. Smith, and M. Zaldarriaga, Non-Gaussianities in single field inflation and their optimal limits from the WMAP 5-year data, *J. Cosmol. Astropart. Phys.* **01** (2010) 028.
- [65] P. A. R. Ade *et al.* (Planck Collaboration), Planck 2013 Results. XXIV. Constraints on primordial non-Gaussianity, *Astron. Astrophys.* **571**, A24 (2014).
- [66] Y. Akrami *et al.* (Planck Collaboration), Planck 2018 results. IX. Constraints on primordial non-Gaussianity, *Astron. Astrophys.* **641**, A9 (2020).
- [67] F. G. Pedro and A. Westphal, Flattened axion monodromy beyond two derivatives, *Phys. Rev. D* **101**, 043501 (2020).
- [68] J. L. Cook and L. Sorbo, Particle production during inflation and gravitational waves detectable by ground-based interferometers, *Phys. Rev. D* **85**, 023534 (2012); **86**, 069901(E) (2012).
- [69] L. Senatore, E. Silverstein, and M. Zaldarriaga, New sources of gravitational waves during inflation, *J. Cosmol. Astropart. Phys.* **08** (2014) 016.
- [70] B. A. Campbell, N. Kaloper, R. Madden, and K. A. Olive, Physical properties of four-dimensional superstring gravity black hole solutions, *Nucl. Phys.* **B399**, 137 (1993).
- [71] N. Barnaby, E. Pajer, and M. Peloso, Gauge field production in axion inflation: Consequences for monodromy, non-Gaussianity in the CMB, and gravitational waves at interferometers, *Phys. Rev. D* **85**, 023525 (2012).
- [72] A. Linde, S. Mooij, and E. Pajer, Gauge field production in supergravity inflation: Local non-Gaussianity and primordial black holes, *Phys. Rev. D* **87**, 103506 (2013).

- [73] V. Domcke, V. Guidetti, Y. Welling, and A. Westphal, Resonant backreaction in axion inflation, *J. Cosmol. Astropart. Phys.* **09** (2020) 009.
- [74] E. V. Gorbar, K. Schmitz, O. O. Sobol, and S. I. Vilchinskii, Gauge-field production during axion inflation in the gradient expansion formalism, *Phys. Rev. D* **104**, 123504 (2021).
- [75] H. V. Ragavendra, P. Saha, L. Sriramkumar, and J. Silk, Primordial black holes and secondary gravitational waves from ultraslow roll and punctuated inflation, *Phys. Rev. D* **103**, 083510 (2021).
- [76] J. Fumagalli, S. Renaux-Petel, and L. T. Witkowski, Oscillations in the stochastic gravitational wave background from sharp features and particle production during inflation, *J. Cosmol. Astropart. Phys.* **08** (2021) 030.
- [77] L. Anguelova, On primordial black holes from rapid turns in two-field models, *J. Cosmol. Astropart. Phys.* **06** (2021) 004.
- [78] Y. Cai and Y.-S. Piao, Intermittent null energy condition violations during inflation and primordial gravitational waves, *Phys. Rev. D* **103**, 083521 (2021).
- [79] I. Dalianis, G. P. Kodaxis, I. D. Stamou, N. Tetradis, and A. Tsigkas-Kouvelis, Spectrum oscillations from features in the potential of single-field inflation, *Phys. Rev. D* **104**, 103510 (2021).
- [80] J. Fumagalli, G. A. Palma, S. Renaux-Petel, S. Sypsas, L. T. Witkowski, and C. Zenteno, Primordial gravitational waves from excited states, *J. High Energy Phys.* **03** (2022) 196.
- [81] Y. Cui and E. I. Sfakianakis, Detectable gravitational wave signals from inflationary preheating, [arXiv:2112.00762](https://arxiv.org/abs/2112.00762).
- [82] C. Caprini and D. G. Figueroa, Cosmological backgrounds of gravitational waves, *Classical Quantum Gravity* **35**, 163001 (2018).
- [83] N. Bartolo *et al.*, Science with the space-based interferometer LISA. IV: Probing inflation with gravitational waves, *J. Cosmol. Astropart. Phys.* **12** (2016) 026.
- [84] K. Yagi and N. Seto, Detector configuration of DECIGO/BBO and identification of cosmological neutron-star binaries, *Phys. Rev. D* **83**, 044011 (2011); **95**, 109901(E) (2017).
- [85] S. Hild *et al.*, Sensitivity studies for third-generation gravitational wave observatories, *Classical Quantum Gravity* **28**, 094013 (2011).
- [86] V. Domcke, F. Muia, M. Pieroni, and L. T. Witkowski, PBH dark matter from axion inflation, *J. Cosmol. Astropart. Phys.* **07** (2017) 048.
- [87] P. Campeti, E. Komatsu, D. Poletti, and C. Baccigalupi, Measuring the spectrum of primordial gravitational waves with CMB, PTA and laser interferometers, *J. Cosmol. Astropart. Phys.* **01** (2021) 012.
- [88] M. Tristram *et al.*, Improved limits on the tensor-to-scalar ratio using BICEP and Planck data, *Phys. Rev. D* **105**, 083524 (2022).
- [89] P. Ade *et al.* (BICEP2, Keck Array Collaborations), BICEP2 / Keck Array x: Constraints on Primordial Gravitational Waves using Planck, WMAP, and New BICEP2/Keck Observations through the 2015 Season, *Phys. Rev. Lett.* **121**, 221301 (2018).
- [90] M. Kamionkowski and J. March-Russell, Planck scale physics and the Peccei-Quinn mechanism, *Phys. Lett. B* **282**, 137 (1992).
- [91] M. Doran, M. J. Lilley, J. Schwindt, and C. Wetterich, Quintessence and the separation of CMB peaks, *Astrophys. J.* **559**, 501 (2001).
- [92] G. Ye and Y.-S. Piao, Is the Hubble tension a hint of AdS phase around recombination?, *Phys. Rev. D* **101**, 083507 (2020).
- [93] G. Ye, B. Hu, and Y.-S. Piao, Implication of the Hubble tension for the primordial Universe in light of recent cosmological data, *Phys. Rev. D* **104**, 063510 (2021).
- [94] E. H. Tanin and T. Tenkanen, Gravitational wave constraints on the observable inflation, *J. Cosmol. Astropart. Phys.* **01** (2021) 053.
- [95] F. Takahashi and W. Yin, Cosmological implications of $n_s \approx 1$ in light of the Hubble tension, [arXiv:2112.06710](https://arxiv.org/abs/2112.06710).
- [96] A. A. Starobinsky, A new type of isotropic cosmological models without singularity, *Phys. Lett.* **91B**, 99 (1980).